

**DAMAGE THRESHOLD OF PLATINUM COATING USED  
FOR OPTICS FOR SELF-SEEDING OF SOFT X-RAY  
FREE ELECTRON LASER**

by

**Jacek Krzywinski<sup>\*</sup>, Daniele Cocco<sup>1</sup>, Stefan Moeller<sup>1</sup>, Daniel Ratner<sup>1</sup>**

*<sup>1</sup>SLAC National Accelerator Laboratory, 2575 Sand Hill Road, Menlo Park, CA 94025,*

*USA*

October 2014

**Abstract:** We investigated the experimental damage threshold of platinum coating on a silicon substrate illuminated by soft x-ray radiation at grazing incidence angle of 2.1 deg. The coating was the same as the blazed grating used for the soft X-ray self-seeding optics of the Linac Coherent Light Source free electron laser. The irradiation condition was chosen such that the absorbed dose was similar to the maximum dose expected for the grating. The expected dose was simulated by solving the Helmholtz equation in non-homogenous media. The experiment was performed at 900 eV photon energy for both single pulse and multi-shot conditions. We have not observed single shot damage. This corresponds to a single shot damage threshold being higher than 3 J/cm<sup>2</sup>. The multiple shot damage threshold measured for 10 shots and about 600 shots was determined to be 0.95 J/cm<sup>2</sup> and 0.75 J/cm<sup>2</sup> respectively. The damage threshold occurred at an instantaneous dose which is higher than the melt dose of platinum.

---

## **1. Introduction**

In recent years, the advent of the Free Electron Laser (FEL) opened up the door to new classes of experiments, including dynamical studies of chemical and physical phenomenon, lens-less diffraction of periodic and non-periodic structures and the study of samples that are suffering radiation damage at third generation x-ray sources. The FEL pulses have very high peak power, ultra-short duration and are produced in a narrow photon bandwidth. In most cases, the radiation is produced by the Self-Amplified Spontaneous Emission (SASE) mechanism. The

SASE-produced radiation suffers poor shot-to-shot reproducibility. The centroid of the energy spectrum jitters, both the spectral and time profiles have poor coherence properties, and the bandwidth of a SASE beam can be of the order of 0.5% (or higher) of the fundamental emitted photon energy. To create a Fourier limited FEL pulse, a couple of approaches were adopted. One of them is direct seeding, where an external laser, emitting a particular wavelength [1] “seeds” the electron beam to create a coherent emission at the same wavelength, but with amplified pulse power. More recently, the Fermi@Elettra team employed a technique called High Gain Harmonic Generation (HG) [2]. In this case, an external laser seeds the electron beam at a particular wavelength, but the radiation is amplified at a shorter wavelength. In both direct seeding and HG, the maximum photon energy is limited by the availability of an external seeding laser with enough power and with proper temporal characteristics at short enough wavelengths. A way to overcome this limit is using the self-seeding scheme, consisting of a monochromator inserted into the undulator chain that generates the SASE beam [3]. After a few undulator sections, a monochromator filters the SASE beam and a photon beam with narrowed photon bandwidth is used to seed the electrons in the downstream undulators. This scheme was successfully demonstrated in the hard x-ray regime at LCLS [4] and is now being implemented in the soft X-ray regime [5, 6].

For the soft X-ray self-seeding (SXRSS) project, the narrow bandwidth of the SASE beam is selected by a diffraction grating based monochromator. The SXRSS project is designed to reach a resolving power  $E/\Delta E$  of 5000 or larger and to fit the monochromator into a single undulator section, just under 4m long. In order to achieve this goal it turned out that the grating should work in fixed incidence mode [6] and should be the very first optical element. The distance from the source to the grating varies from 3m to 8m depending on photon energy and undulator configuration.

It is expected that a  $B_4C$  coated grating would have a higher damage threshold than the platinum coating. However, it is known that mirrors working in x-ray regime suffer from carbon contamination. Carbon contaminated  $B_4C$  based optics cannot be cleaned by oxygen methods as the cleaning process damages  $B_4C$  material. By contrast, platinum-coated optics can be cleaned from the carbon contamination in-situ [7]. Therefore we decided to pursue the platinum coated grating solution and test damage of platinum coatings in the soft x-ray regime.

The reason to perform the tests is the absence of damage studies at the photon energies at which we plan to work (500-1200 eV) and the difficulty to predict the behaviors of thin films deposited on a substrate. There are several studies carried out in the UV and at normal incidence but very few studies were performed at grazing incidence and none in the soft X-ray region. Therefore, the damage resistance to a highly energetic soft X-ray beam of a metallic thin film deposited on a substrate (Silicon in our case) is almost unexplored. The planned photon energy for the initial commissioning of the SXRSS was around 900 eV, and we decided to concentrate our studies on this particular value.

## **2. Experimental**

### *2.1 Experimental setup*

The measurements were carried out at the SXR instrument at LCLS. A detailed description of this instrument and its beamline components are given elsewhere [8]. Here we only give a brief overview and schematics in Fig. 1, which is relevant to this study. The FEL beam produced in the undulator traverses the Front End Enclosure (FEE) which houses a gas attenuator and the gas detectors that measure the pulse energy of the FEL beam for each pulse [9]. Before the beam reaches the SXR beamline it is reflected off the soft x-ray offset mirrors

(SOMS) and directed into the SXR beamline. The beamline consists of a monochromator which can be operated in zeroth order by reflecting off the unruled area of the grating or in a monochromatic mode. After the exit slit of the monochromator a gas detector (GMD) measures the average and shot by shot pulse energy [10].

A Kirkpatrick-Baez (KB) refocusing mirror pair can change the beam size on the sample. The sample was mounted in the monitor tank downstream of the experimental chamber which also houses YAG screens to view the beam spot. The sample was mounted on a rotatable manipulator and was pre-aligned to the FEL beam coordinates to an accuracy of better than 0.1 degrees.

The LCLS photon energy was tuned to 900eV and the monochromator was operated in zeroth order. The FEL pulse energy was measured by the FEE gas detectors afor each pulse. The transmission of the KB mirrors has been characterized previously to be around 50%.

The beam size was monitored using a Ce:YAG sample mounted on the same sample holder and adjusted to 30 – 40  $\mu\text{m}$  with the bendable KB mirror system and left at this position during the irradiation. The fluence was controlled via the adjustable gas attenuator pressure.

An Opal camera mounted at the end of a microscope allowed for online monitoring of the sample during the irradiation.

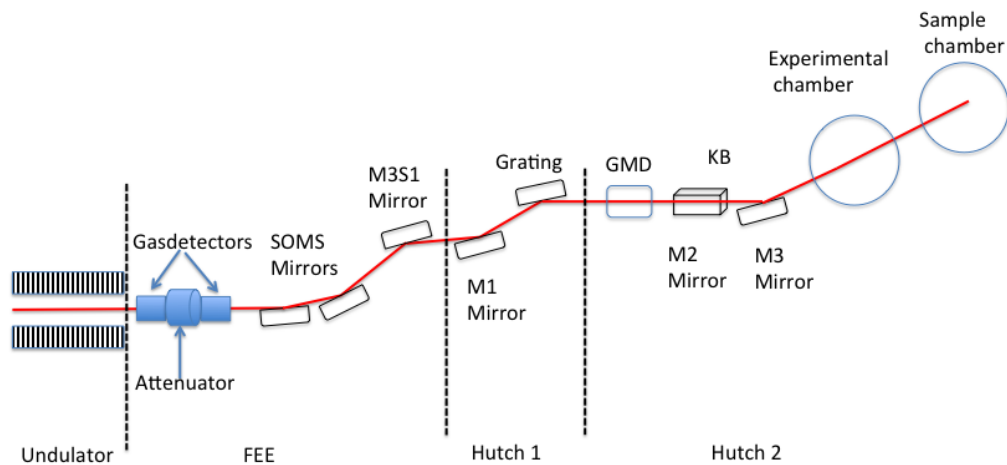


Fig. 1. Schematic lay-out of the SXR beamline: Front End enclosure (FEE) with diagnostics and Soft X-ray offset Mirrors (SOMS) and M3S1 mirror, Hutch 1 contains the monochromator (mirror M1 and grating) and hutch 2 the Gas Monitor Detector (GMD) and focusing (KB) optics. The sample was mounted in the sample chamber located after the experimental chamber.

## 2.2 Sample

The irradiated sample was a 60X20X5 mm silicon substrate with a single layer of 51 nm (+/- 0.15 nm) of platinum deposited on the surface via sputtering (by Incoatec gmbh). No binding layer or adhesive layer was used to increase the adhesion of Pt to the silicon substrate. The

measured micro roughness was below 0.5 nm rms, good enough to detect any damage induced to the optical surface by the radiation.

### 2.3 Determination of the maximum fluence at normal incidence

The measurement of the maximum fluence of a non-Gaussian beam involves two steps: pulse energy measurements and determination of the so called effective area  $A_{eff}$  [11, 12] of the focused beam. The effective area  $A_{eff}$  is defined as:

$$A_{eff} = \iint_S F(x, y) / F_{max} dx dy = Ep / F_{max}$$

where  $F(x,y)$  is the fluence distribution,  $F_{max}$  the maximum fluence and  $Ep$  the pulse energy. The effective area  $A_{eff}$  establishes a simple relationship between the maximum fluence  $F_{max}$  and the photon pulse energy  $Ep$ :  $F_{max}=Ep/A_{eff}$ . Pulse energy was measured by a gas detector described in details elsewhere [13]. The effective area  $A_{eff}$  was derived from the fluence distribution  $F(x,y)$  measured by the imprints method [12]. We have used a polished  $PbWO_4$  crystal as a target for imprints. Series of imprints were done at different pulse energy levels  $Ep$  and analyzed in a way described in [12]. An image of a typical imprint is presented in Fig. 2.



Fig. 2. An image of a typical imprint in the  $PbWO_4$  target. In this particular case the maximum fluence was twice higher than the damage threshold in the  $PbWO_4$ .

Our experiment was carried out in two different days, at two different focusing conditions corresponding to two different effective areas measured as  $560 \mu m^2$  and  $1200 \mu m^2$ .

### 2.4 Irradiation at grazing incidence

The irradiation conditions for the grazing incidence case were chosen such that the absorbed dose was similar or higher than the maximum dose expected for the blazed grating used in the optical system for the SXRSS project. The expected dose was simulated by solving the Helmholtz equation in non-homogenous media, which will be described in more details in section 3. The simulations showed that, to have a comparable dose, the angle of incidence should be 2.1 degrees.

We have performed single shot and multi-shot irradiations for 10 and about 600 shots at different pulse energy levels. The pulse energy was controlled by changing the gas pressure in a gas attenuator. The average incoming FEL pulse energy, before the gas attenuator, was on the order of 1 mJ. More precisely, after having measured each single shot per irradiated area

we determined the average pulse energy for the first study to be 1.07mJ and for the second study to be 0.98mJ

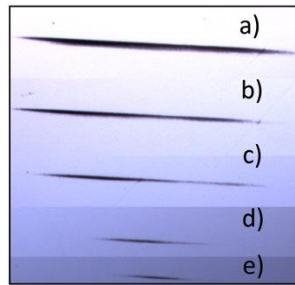


Fig. 3 Images of damage of the Pt coating caused by the focused x-ray beam at grazing incidence of 2 degrees. Different images correspond to different pressures of the gas attenuator: a) 0.6 Tr, b) 0.7 Tr, c) 0.8Tr, d) 0.9 Tr and e) 1Tr

For each attenuation level we irradiated two separate sample locations by moving the sample to a fresh spot. We changed the transmission of the beam line, by changing the pressure of the gas, over the range 0.07 – 3.5%, corresponding to pulse energy on the sample from 0.7 to 35  $\mu$ J. This attenuation range was sufficient to observe the damage threshold for multi-shot irradiations. As it turned out after the experiment we were not able to detect single shot damage in this attenuation range.

### 3. Simulations

In our simulations we used a beam propagation method to solve the Helmholtz equation in inhomogeneous media [14, 15]. This type of simulation explained the results of damage experiment for carbon coated lamellar grating performed at FLASH facility [15]. Fig 4 shows simulation of distribution of absorbed energy density  $e_d$  in the blazed silicon grating coated with 50 nm thick Pt layer. The simulation shows that the specific field distribution at the surface leads to an enhancement of the absorbed energy at the edge of the blazed grating structure illuminated at 1 deg incident angle. The maximum value of  $e_d$  is about 20% lower than the  $e_d$  calculated for the flat surface illuminated by the beam at 2.1 deg grazing incident angle. This angle corresponds to the angle between the incident beam and the grating's facets. Therefore, to mimic this situation we have chosen in our experiment 2 degrees as the incident angle. The simulations also show that the dependence of the absorbed energy on the photon energy in the range 200 eV - 1200 eV is rather weak with a flat maximum around 800 eV (see Fig 4). Therefore one can expect that the results obtained for the photon energy of 900 eV, used in our experiment, are also representative for a larger photon energy range.

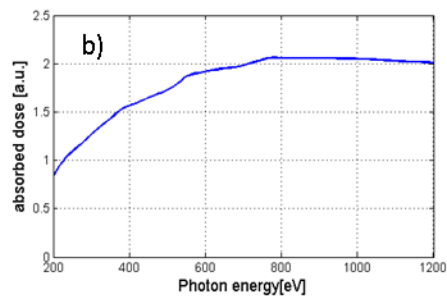
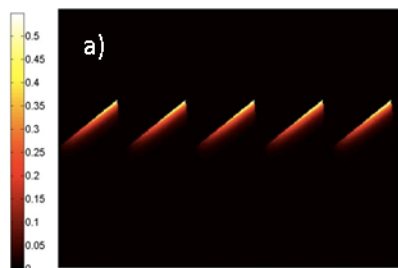


Fig. 4 a) Simulated distribution of absorbed energy density  $e_d$  in the blazed silicon grating coated with 50 nm thick Pt layer. The grating is illuminated at 1 degree grazing incident angle. b) Dependence of maximum of absorbed energy density  $e_d$  as a function of photon energy.

#### 4. Data analysis and results

The damage threshold at grazing incidence was determined as follows. First the area of the damaged spots was plotted as a function of attenuator pressure (Fig.5). The pressure is proportional to the logarithm of the transmission of the beamline. This plot relates to the so called Liu plot [16] which is often used in damage threshold analysis.

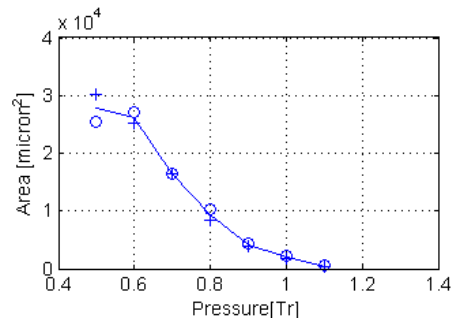


Fig. 5. The area of the damaged spots as a function of the attenuator pressure for the second set of exposures. Crosses and circles represent two different repetition of using the same irradiation conditions.

We used linear regression and the last three points on the plot to calculate the pressure  $P_{th}$  at which the damage would vanish. The damage threshold is then determined as  $F_{th} = E_{th}/A_{eff}$  where  $E_{th}$  is the transmitted energy corresponding to  $P_{th}$ .

As it has been mentioned above we did two series of multishot irradiations applying 10 shots and 600 shots. The focusing conditions for these two series were characterized by measured effective area of the spots of  $1200 \mu\text{m}^2$  and  $560 \mu\text{m}^2$  respectively. The determined damage thresholds are different in the two cases. They were  $0.75 \text{ J/cm}^2$  and  $0.95 \text{ J/cm}^2$  for the 600 shots case and 10 shots case respectively. One can observe that the lower damage threshold corresponds to larger number of shots.

The maximum combined uncertainty in our measurement is about 35% and is due to the individual uncertainties in determining the attenuator pressure threshold values at 0.5%, measuring the effective area at 10%, and determining the overall transmission at 20%, and the pulse energy measurement at 5%.

Surprisingly, our focusing and transmission conditions did not produce any single shot damage. We did not have on-line high resolution microscope to realize during experiment that single shot damage was not happening. Therefore we can only state that we were not able to detect any single shot damage and that the threshold is higher than  $3 \text{ J/cm}^2$ . We intend to reinvestigate the single shot damage threshold in future studies.

## 5. Discussion

The key quantity that helps to assess the damage is the instantaneous absorbed dose per atom at the mirror surface:

$$D_{atom} = \frac{F(1-R) \cdot \sin(\theta)}{d \cdot \rho_{atom}}$$

where  $F$  is the fluence,  $R$  is the reflectivity,  $\theta$  is the grazing incidence angle,  $\rho_{atom}$  is the number of atoms per unit volume,

$$d = -\frac{\lambda}{4\pi \cdot \text{Im} \left[ n \cdot \sqrt{1 - (\cos(\theta) / n)^2} \right]}$$

is the complex refractive index.

The calculated absorbed dose for the damage thresholds  $0.75 \text{ J/cm}^2$  and  $0.95 \text{ J/cm}^2$  corresponds to  $6 \text{ eV/atom}$  and  $8 \text{ eV/atom}$  respectively. These dose values can be compared with the energy density  $D_{melt}$  which is required to bring a solid to the melt temperature. In the case of platinum  $D_{melt} \approx 0.47 \text{ eV/atom}$ . This value is close to the experimental single shot damage value of  $0.51 \text{ eV/atom}$  measured for bulk platinum sample at hard X-rays [17].

Clearly, a significant amount of absorbed energy is transported away from the surface before it melts. A simplified picture of what happens when the surface of a solid is excited by a femtosecond X-ray pulse can be viewed within the so called two temperature model [18] describing separately electron and ion systems that are coupled thermally by an energy transfer mechanism, e.g. by the electron – phonon coupling. The heat diffusion is also modeled individually in the two subsystems with appropriate thermal conductivity models. In addition to thermal diffusion the ballistic transport of electrons can be also taken into account [19]. The typical ion – electron temperature equilibration times, measured for metals, are in order of  $1 \text{ ps} - 30 \text{ ps}$  depending on the ion atomic weight and electron-phonon coupling strength. It is known from experiments performed for metals using femtosecond optical pulses that during this time the electron system can transport the energy far beyond the absorption layer [19]. As a result the maximum ion temperature of the surface measured in pump-and probe experiments were lower than expected when assuming thermal equilibrium in the absorption layer.

Recent damage experiment done at grazing incidence with  $10 \text{ keV}$  photons [20] also indicated that the electrons transported energy away from the absorption region before it melts. In this work authors concluded that in order to explain the measured damage thresholds the energy deposition length should be about  $30 \text{ nm}$  compared to  $2 \text{ nm}$  absorption length. The energy deposition length was attributed to the electron collisional range [21] and the thermal diffusion was not considered.

For the grazing incidence angle of  $2.1 \text{ deg}$  the calculated absorption length  $d$  of  $1.7 \text{ nm}$  is much smaller than the thickness of the coating of  $50 \text{ nm}$ . The calculated instantaneous absorption dose is approximately 14 times larger than the melt dose. Therefore one can

conclude that the energy deposition range of  $\sim 24$  nm should be also approximately 14 times longer than the absorption length.

Our results and the results reported in [20] are very important for development of metal coated optics that is exposed to intense, ultrashort X-ray pulses. Understanding the energy transport process can help to design optics which can withstand higher instantaneous power and optimize scientific instruments at XFELs.

### Acknowledgments

The authors would like to thank M. Holmes, G. Gassner, SXR Instrument and SLAC Metrology teams for their help during the beam time. Work supported by Department of Energy contract DE-AC02-76SF00515.

---

### References and links

1. L. H. Yu "Generation of intense UV radiation by sub harmonically seeded single-pass free-electron lasers" *Phys. Rev. A*, Vol. 44, pp. 5178–5193 (1991)
2. E. Allaria, C. Callegari, D. Cocco, W. M. Fawley, M. Kiskinova, C. Masciovecchio, F. Parmigiani, "The FERMI@Elettra free-electron-laser source for coherent x-ray physics: photon properties, beam transport system and applications" *New Journal of Physics* 12 (2010) 075002
3. J. Feldhaus, E. L. Saldin, J. R. Schneider, E. A. Schneidmiller, and M. V. Yurkov, "Possible application of X-ray optical elements for reducing the spectral bandwidth of an X-ray SASE FEL," *Opt. Commun.* 140, 341–352 (1997)
4. J. Amann, W. Berg, V. Blank, F.-J. Decker, Y. Ding, P. Emma, Y. Feng, J. Frisch, D. Fritz, J. Hastings, Z. Huang, J. Krzywinski, R. Lindberg, H. Loos, A. Lutman, H.-D. Nuhn, D. Ratner, J. Rzepiela, D. Shu, Yu. Shvyd'ko, S. Spampinati, S. Stoupin, S. Terentyev, E. Trakhtenberg, D. Walz, J. Welch, J. Wu, A. Zholents, D. Zhu. "Demonstration of self-seeding in a hard-X-ray free-electron laser" *Nature Photonics* 6, 693-698 (2012)
5. Y. Feng, J. Amann, D. Cocco, C. Field, J. Hastings, P. Heimann, Z. Huang, H. Loos, J. Welch, J. Wu, K. Chow, P. Emma, N. Rodes, R. Schoenlein, "System design for Self-Seeding the LCLS at Soft X-Ray Energies" *Proc. FEL 2012 conference*, Nara, Japan (2012)
6. D. Cocco, R. Abela; J.W. Amann, K. Chow, P.J. Emma; Y. Feng; G.L. Gassner, J. Hastings; P. Heimann, Z. Huang, H. Loos, P.A. Montanez; D. Morton; H-D. Nuhn; D. F. Ratner, L.N. Rodes, U. Flechsig, J. Welch, J. Wu., "The optical design of the soft x-ray selfseeding at LCLS ", *Proc. SPIE* 8849, 88490A (September 30, 2013); doi:10.1117/12.2024402
7. T. Koide, H. Fukutani, M. Yanagihara, Y. Aiura, S. Sato, T. Shidara, H. Fukutani A. Fujimori, M. Niwano, and H. Kato, "Resuscitation of carbon-contaminated mirrors and gratings by oxygen-discharge cleaning. in the 4-40-eV range" *Appl Opt.* 1987 Sep 15; 26(18): 3884-94. doi: 10.1364/AO.26.003884.
8. W. Schlotter, J. Turner, M. Rowen, P. Heimann, M. Holmes, O. Krupin, M. Messerschmidt, S. Moeller, J. Krzywinski, R. Soufli, M. Fernández-Perea, N. Kelez, S. Lee, R. Coffee, G. Hays, M. Beye, N. Gerken, F. Sorgenfrei, S. Hau-Riege, L. Juha, J. Chalupsky, V. Hajkova, A. Mancuso, A. Singer, O. Yefanov, I.A Vartanyants, G. Cadenazzi, B. Abbey, K.A Nugent, H. Sinn, J. Lüning, S. Schaffert, S. Eisebitt, W. Lee, A. Scherz, A. Nilsson, W. Wurth, "The Soft x-ray instrument for materials studies at



the linac coherent light source x-ray free electron laser” Rev. Sci. Instrum. 83, 043107 (2012), doi: 10.1063/1.3698294

9. S. Moeller, J. Arthur, A. Brachmann, R. Coffee, F.-J. Decker, Y. Ding, D. Dowell, S. Edstrom, P. Emma, Y. Feng, A. Fisher, J. Frisch, J. Galayda, S. Gilevich, J. Hastings, G. Hays, P. Hering, Z. Huang, R. Iverson, J. Krzywinski, S. Lewis, H. Loos, M. Messerschmidt, A. Miahnahri, H.-D. Nuhn, D. Ratner, J. Rzepiela, D. Schultz, T. Smith, P. Stefan, H. Tompkins, J. Turner, J. Welch, B. White, J. Wu, G. Yocky, R. Bionta, E. Ables, B. Abraham, C. Gardener, K. Fong, S. Friedrich, S. Hau-Riege, K. Kishiyama, T. McCarville, D. McMahon, M. McKernan, L. Ott, M. Pivovarov, J. Robinson, D. Ryutov, S. Shen, R. Soufli, and G. Pile, “Photon Beamlines and Diagnostics at LCLS,” Nucl. Instrum. Methods Phys. Res. A635(1), S6–S11 (2011)
10. K. Tiedtke, A. Azima, N. von Bargaen, L. Bittner, S. Bonfigt, S. Düsterer, B. Faatz, U. Frühling, M. Gensch, Ch. Gerth, N. Guerassimova, U. Hahn, T. Hans, M. Hesse, K. Honkavaar, U. Jastrow, P. Juranic, S. Kapitzki, B. Keitel, T. Kracht, M. Kuhlmann, W. B. Li, M. Martins, T. Nunez, E. Plönjes, H. Redlin, E. L. Saldin, E. A. Schneidmiller, J. R. Schneider, S. Schreiber, N. Stojanovic, F. Tavella, S. Toleikis, R. Treusch, H. Weigelt, M. Wellhöfer, H. Wabnitz, M. V. Yurkov, and J. Feldhaus, “The soft x-ray free-electron laser FLASH at DESY: beamlines, diagnostics and end-stations,” New J. Phys.11, 023029 (2009).
11. ISO 11254-1:2000, IOS Publications, Geneva, (2000)
12. J. Chalupský, J. Krzywinski, L. Juha, V. Hájková, J. Cihelka, T. Burian, L. Vyšín, J. Gaudin, A. Gleeson, M. Jurek, A. R. Khorsand, D. Klingner, H. Wabnitz, "Spot size characterization of focused non-Gaussian X-ray laser beams", Opt. Express 18, 27836 (2010)
13. K. Tiedtke, A. A. Sorokin, U. Jastrow, P. Juranić, S. Kreis, N. Gerken, M. Richter, U. Arp, Y. Feng, D. Nordlund, R. Soufli, M. Fernández-Perea, L. Juha, P. Heimann, B. Nagler, H. J. Lee, S. Mack, M. Cammarata, O. Krupin, M. Messerschmidt, M. Holmes, M. Rowen, W. Schlotter, S. Moeller, and J. J. Turner, “Absolute pulse energy measurements of soft x-rays at the Linac Coherent Light Source”, Optics Express, Vol. 22, Issue 18, pp. 21214-21226 (2014)
14. O.K. Ersoy, “Diffraction, Fourier optics and Imaging”, A John Wiley & Sons, Inc., Publication (2007)
15. J. Gaudin, C. Ozkan, J. Chalupský, S. Bajt, T. Burian, L. Vyšín, N. Coppola, S. Farahani, H. Chapman, G. Galasso, V. Hájková, M. Harmand, L. Juha, M. Jurek, R. A. Loch, S. Möller, M. Nagasono, M. Störmer, H. Sinn, K. Saksl, R. Sobierajski, J. Schulz, P. Sovak, S. Toleikis, K. Tiedtke, T. Tschentscher, and J. Krzywinski, “Investigating the interaction of x-ray free electron laser radiation with grating structure” Optics Letters, Vol. 37, Issue 15, pp. 3033-3035 (2012)
16. J. Liu, “Simple technique for measurements of pulsed Gaussian-beam spot sizes” Opt. Lett. 7, 196 (1982)
17. Koyama, T., Yumoto, H., Senba, Y., Tono, K., Sato, T., Togashi, T., Inubushi, Y., Katayama, T., Kim, J., Matsuyama, S., Mimura, H., Yabashi, M., Yamauchi, K., Ohashi, H., and Ishikawa, T., "Investigation of ablation thresholds of optical materials using 1- $\mu$ m-focusing beam at hard X-ray free electron laser," Opt. Express 21, 15382 (2013)
18. I. Anisimov, B.L. Kapeliovich, T.L. Perel'man, Sov. Phys. JETP 39 (1974) 375
19. J. Hohlfeld et al. “Electron and lattice dynamics following optical excitation of metals”, Chemical Physics 251 \_2000. 237–258
20. T.Koyama, H.Yumoto, K.Tono, T.Sato, T.Togashi, Y.Inubushi, T.Katayama, J.Kim, S.Matsuyama, H.Mimura, M.Yabashi, K.Yamauchi, H.Ohashi, “Damage threshold

investigation using grazing incidence irradiation by hard X-ray free electron laser" Proc. SPIE 8848, 88480T , (2013)

21. Kobetich, E. J., and Katz, R., "Energy Deposition by Electron Beams and  $\delta$  Rays," Phys. Rev. 170, 391-396 (1968).